Manuscript submitted March 26, 1987; revised manuscript received Aug. 12, 1987.

Clarkson University assisted in meeting the publication costs of this article.

REFERENCES

1. E. B. Budevski, in "Comprehensive Treatise of Electrochemistry," B. E. Conway, J. O'M Bockris, E. Yeager, S. U. M. Khan, and R. E. White, Editors Vol. 7, pp. 399-450, Plenum Press, New York (1983).
2. S. Toshev, A. Milchev, and S. Stoyanov, *J. Cryst. Growth*, **13/14**, 123 (1972).
3. A. Milchev and S. Stoyanov, *J. Electroanal. Chem.*, **72**, 33 (1976).
4. A. Milchev, *Electrochim. Acta*, **28**, 947 (1983).
5. I. Markov, *ibid.*, **28**, 959 (1983).
6. A. Milchev, *ibid.*, **28**, 941 (1983).
7. N. Pangarov, *ibid.*, **28**, 763 (1983).
8. V. Bostanov, W. Obretenov, G. Staikov, and E. Budevski, *J. Electroanal. Chem.*, **146**, 303 (1983).
9. A. Milchev, *J. Chem. Phys.*, **78**, 1994 (1983).
10. M. Fleischmann, D. J. Lax, and H. R. Thirsk, *Trans. Faraday Soc.*, **64**, 3137 (1968).
11. R. D. Armstrong and J. A. Harrison, *This Journal*, **116**, 328 (1969).
12. R. D. Armstrong and A. A. Metcalfe, *J. Electroanal. Chem.*, **71**, 5 (1976).
13. W. Davison and J. A. Harrison, *ibid.*, **44**, 213 (1973).
14. P. Bindra, M. Fleischmann, J. W. Oldfield, and D. Singleton, *Faraday Discuss. Chem. Soc.*, **56**, 180 (1974).
15. G. Hills, A. K. Pour, and B. Scharifker, *Electrochim. Acta*, **28**, 891 (1983).
16. M. Y. Abyaneh and M. Fleischmann, *J. Electroanal. Chem.*, **119**, 197 (1981).
17. M. Y. Abyaneh and M. Fleischmann, *ibid.*, **119**, 187 (1981).
18. B. Scharifker and G. Hills, *Electrochim. Acta*, **28**, 879 (1983).
19. A. Scheludko and M. Todorova, *Bull. Acad. Sci. Bulg. (Phys.)*, **3**, 61 (1952).
20. R. Kaischew and B. Mutaftschev, *Electrochim. Acta*, **10**, 643 (1965); *Z. Phys. Chem.*, **204**, 334 (1955).
21. T. Hepel, F. H. Pollak, and W. E. O'Grady, Submitted to *J. Electroanal. Chem.*
22. P. Bindra, H. Gerischer, and D. M. Kolb, *This Journal*, **124**, 1012 (1977).
23. T. Hepel, F. H. Pollak, and W. E. O'Grady, *ibid.*, **131**, 2094 (1984).
24. T. Hepel, F. H. Pollak, and W. E. O'Grady, *J. Electroanal. Chem.*, **188**, 281 (1985).
25. T. Hepel, F. H. Pollak, and W. E. O'Grady, *This Journal*, **133**, 69 (1986).
26. Y. S. Huang, H. L. Park, and F. H. Pollak, *Mater. Res. Bull.*, **17**, 1305 (1982).
27. M. Y. Abyaneh, *Electrochim. Acta*, **27**, 1329 (1982).
28. V. Bostanov, R. Roussinova, and E. Budevski, *Chem. Ing. Techn.*, **45**, 179 (1973).
29. E. Budevski, in "Progress in Surface and Membrane Science," Vol. 11, p. 71, Academic Press, New York (1976).

Modeling of Bipolar Semiconductor Photoelectrode Arrays for Electrolytic Processes

S. Cervera-March, E. S. Smotkin, A. J. Bard,* A. Campion, M. A. Fox,* T. Mallouk,* S. E. Webber, and J. M. White

Department of Chemistry, The University of Texas, Austin, Texas 78712

ABSTRACT

The effect of light flux, redox couple concentration, and the number of panels on the electrical and chemical efficiency of a bipolar semiconductor photoelectrode array has been examined using a model based on the power characteristic curves of a single photoelectrochemical cell and the current-voltage characteristics of any desired electrolytic process. Data from a single bipolar CdSe//CoS photoelectrode were used to simulate water splitting array performance under a variety of conditions. Experimental data from a 6 photopanel array were consistent with the simulated results. The optimum number of panels was shown to be independent of light intensity over a range of 0.1-1 AM2 and of the concentration of polysulfide in the interior of the arrays from 0.1 to 1*M*. The efficiency of the CdSe/CoS array for electrical generation (after correcting for light absorption due to the electrolyte) is about 6%.

Recent papers from this laboratory described bipolar semiconductor photoelectrode (BSP) arrays and their application to light-driven water splitting and electrical power generation (1, 2). The term bipolar electrode refers to a configuration consisting of a n- or p-type semiconductor surface in ohmic contact with a dark catalytic electrode surface that serves as the counterelectrode to the facing semiconductor of the next bipolar electrode. These electrodes can be used in a wireless series configuration array to provide sufficiently high voltages to drive electrolytic reactions of interest. The principles of such an array are shown in Fig. 1A. These arrays obviate two problems: (*i*) the location of the semiconductor bandedges relative to the water decomposition potentials and (*ii*) the requirement of semiconductor stability during photohole generation and oxygen production in aqueous solution.

Studies of water photoelectrolysis ("water splitting") date from the work of Honda and Fujishima working with TiO_2 and Pt electrodes (3). The inadequate photopotential generated at the TiO_2/solution interface required the application of an external bias and hence the expenditure of energy in addition to the incident radiant energy. An alternative strategy involves series arrays of PEC cells. The basic principles of PEC devices have been discussed in detail (4-7). In bipolar semiconductor photoelectrodes, vectorial charge transfer occurs: photogenerated minority carriers move to the semiconductor surface and majority carriers move to the electrocatalytic surface. This arrangement optimizes light collection and obviates the need for connecting wires. With five n-TiO_2//Pt (where // represents an ohmic contact) (1) BSP's in series, hydrogen was evolved at the Pt surface of panel 1 with oxygen evolution on the n-TiO_2 surface of panel 5 (1). The electrodes on the inside panels behaved as photovoltaic cells and carried out a regenerative reaction (in this case photoproduction and reduction of oxygen) to provide a bias for the end electrodes. This initial version of the BSP array suffered from the requirement of contact of the end photoanodic semiconductor surface (electrode 1 in Fig. 1) with the solution where O_2 is evolved, thereby limiting the BSP material to large bandgap semiconductors stable under conditions where photogenerated holes oxidize water. However, a (dark) electrocatalytic electrode can be used on the anodic (O_2-evolution) end, instead of the n-type semiconductor, removing this need for semiconductor stability (Fig. 1B). The anodic side of the dark bipolar electrode 1 should be composed of an electrocatalyst for oxygen evolution on the substrate of choice, while the cathodic side is an electrocatalyst appropriate for the redox couple (O/R) used in the BSP array. In these arrays, the illuminated array of

*Electrochemical Society Active Member.

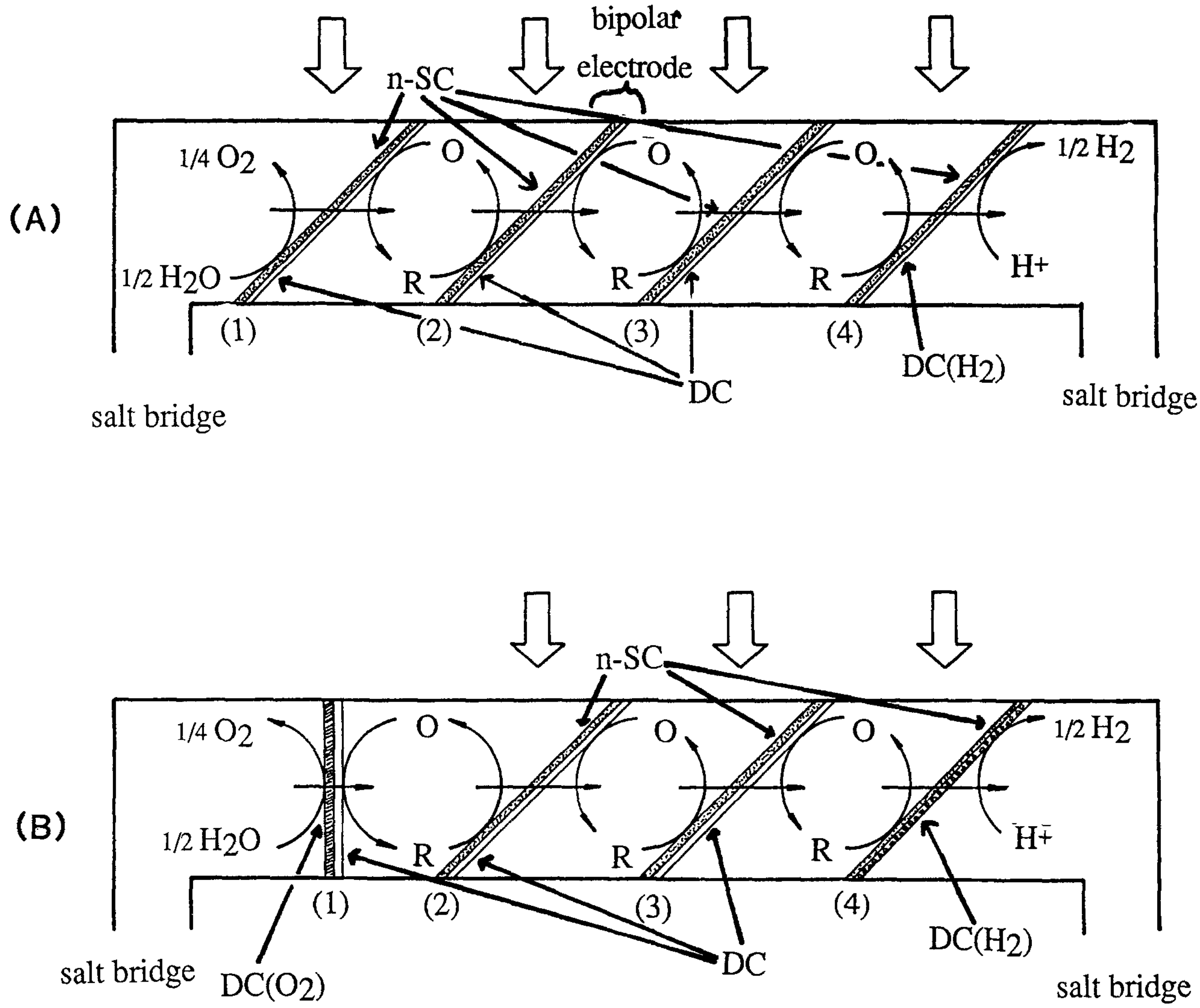

Fig. 1. (A) Initial version of BSP array with end photoanodic surface 1 in contact with solution where oxygen is evolved. n-SC = n-semiconductor; DC = dark electrocatalyst (O → R); DC(H_2) = dark electrocatalyst for H_2 evolution. (B) Small bandgap version with dark bipolar electrode 1. DC(O_2) dark electrocatalyst for oxygen evolution.

BSP's induce a potential in the end dark bipolar electrode. This electrode completes isolation of all BSP semiconductor surfaces from the end solution, permitting the use of any desired redox couple in the interior of the array. The terminal BSP should have a cathodic surface tailored for hydrogen evolution on the cathodic end solution of choice. The interior BSP electrodes should have cathodic surfaces tailored for the redox couple of choice. Thus, an n-type BSP array contains three types of electrodes: (*i*) a terminal dark bipolar electrode with an anodic catalytic surface for oxygen evolution and a cathodic catalytic surface tailored to the redox couple of choice; (*ii*) interior BSP electrodes, where the anodic side is an illuminated semiconductor; and (*iii*) a terminal BSP electrode, where the cathodic side is appropriate for hydrogen evolution. The construction of such a BSP array is shown in Fig. 2. [Alternatively, a p-type array can be fabricated using a semiconductor such as p-GaAs. In such a case, the dark bipolar electrode (B/C) would be on the cathodic side of the array with the direction of electron flow the reverse of that in an n-type array.] In a preliminary letter, we described the above arrangement where illuminated CdSe, a small bandgap semiconductor (1.8 eV), was used to photolyze water yielding separated products of hydrogen and oxygen in a stoichiometric ratio with minimal decomposition of the semiconductor surface (2). The three electrode types comprising the CdSe BSP array are: (*i*) Pt//CoS, (*ii*) CdSe//CoS, (*iii*) CdSe//Pt [where CoS is a (dark) electrocatalyst for polysulfide reduction].

We present here a model of BSP arrays with experimental data describing the relationship between the water

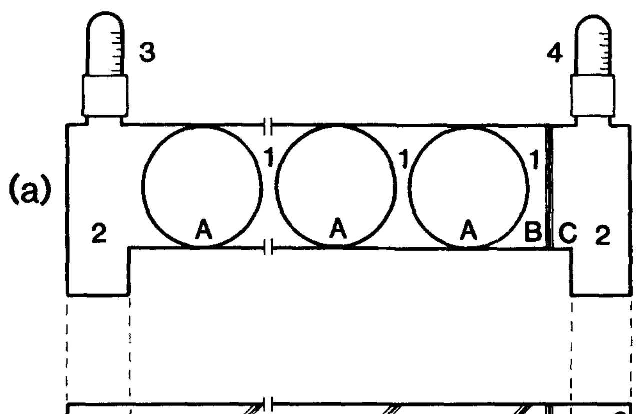

Fig. 2. Pictorial representation of a water photoelectrolysis cell: (a) Side view; (b) top view. Experimental n-CdSe//CoS array. Electrodes: A, CdSe; B, CoS; C, D, Pt. Solutions: 1, 1*M* Na_2S, 1*M* S, 2*M* NaOH; 2, 2*M* KOH. Gas collectors: 3, hydrogen; 4, oxygen. Conceptualized p-type array. A, p-GaAs; B, catalytic surface for reduction of I_3^-; C, D, Pt. Solutions B: 1, 0.25*M* I_3^-; 0.75*M* I^-; 2, 2*M* KOH. Oxygen collected in 3, hydrogen collected at 4.

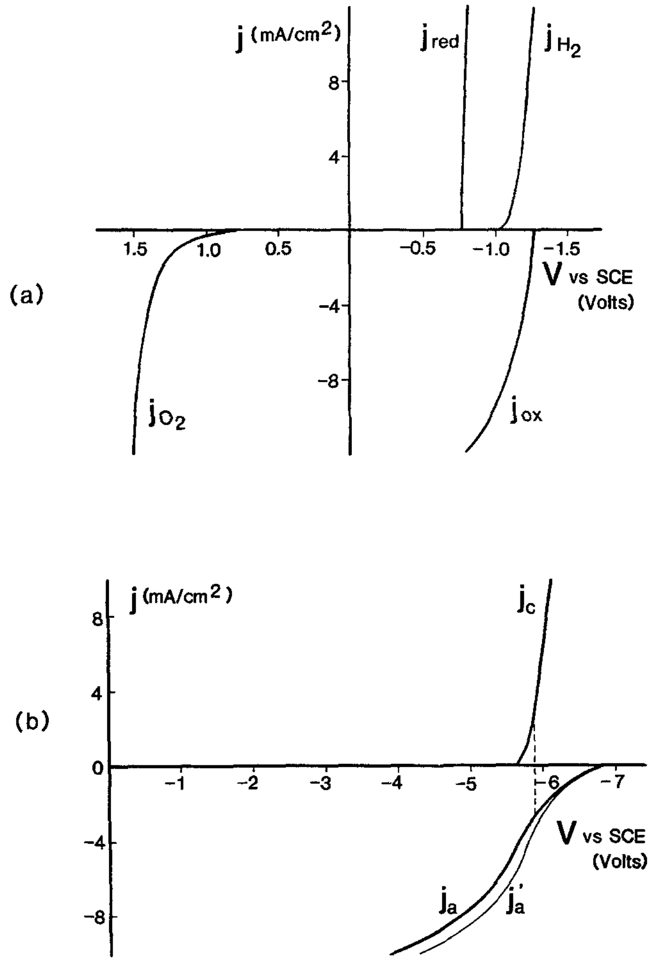

Fig. 3. (a) Current-potential characteristics of a CdSe//CoS PEC in 1:1:1M. NaOH:S:Na$_2$S solution. Curve j_{red} corresponds to the dark reduction: $S_2^{2-} + 2e^- \rightarrow 2S^{2-}$. Curve j_{ox} corresponds to the photo-oxidation: $2S_2^{2-} + 2h^+ \rightarrow S_2^{2-}$. Curves j_{H_2} and j_{O_2} are hydrogen and oxygen evolution on platinum electrodes, in 2M KOH, respectively. Effective solar flux: 67 mW/cm^2. (b) Cathodic and anodic waves for a BSP array with 6 photopanels. Curve j_C: sum of six j_{red} and j_H. Curve j_a: sum of six j_{ox} and $j_o \cdot j_a$ includes internal resistances and bridge resistance of experimental array.

splitting efficiency and electrical power efficiency and how these quantities depend on the number of panels, the overpotentials of the electrodes involved in gas generation, light intensity and redox couple concentrations. Similar analysis for the electrolysis of water using solid-state devices have been presented; see, for example, Pleskov *et al.* (9). We then analyze experimental data for the CdSe-based array based on the model.

Principles of Operation

The curves j_{red} and j_{ox} in Fig. 3a define the electrical characteristics of a CdSe//CoS photoelectrochemical cell with polysulfide (1*M* Na$_2$S, 1*M* S, 1*M* NaOH) as the interior redox couple (2) and the Pt/Na$^+$OH$^-$ interfaces. Current density-potential (j-V) curves for four different processes are given: S^{2-} photo-oxidation on CdSe (j_{ox}); S_x^{2-} reduction (written for simplicity as S_2^{2-}) on CoS (j_{red}); water reduction on Pt (j_{H_2}); water oxidation on Pt (j_{O_2}). The open-circuit voltage (V_{oc}), short-circuit current (i_{sc}), and power curves for the interior cells are calculable from j_{red} and j_{ox}. As described previously (1), for a BSP array system, the cathodic current for H$_2$ evolution, j_c, is obtained by addition of the potentials required for a given j_{H_2} to integer multiples of the potentials required for j_{red} to generate the same currents, where the integer represents the number of BSP's in series. Similarly, from j_{O_2} and j_{ox}, the anodic current, j_a, is obtained (Fig. 3b). Photocell internal resistances are included in the j_{red} wave. With good catalytic cathodes, the wave is linear with a slope depending on the cell resistances. The resistance through the external bridge can be measured or calculated and included in j_a (j_a' is the anodic current without inclusion of the bridge resistance). The operational current density for water splitting ($N = 6$), (where N is the number of panels) is indicated by the dotted line in Fig. 3b, where the cathodic and anodic currents are equal in magnitude.

Another approach is illustrated in Fig. 4. Curve j_R is the power characteristics of a single PEC derived from curves j_{red} and j_{ox} in Fig. 3a by connecting points of equal anodic and cathodic currents to find the corresponding points of the power characteristics. At the point of maximum power, where curve j_R contacts the vertice of rectangle A, $d(j_R \cdot V)/dV = 0$, or

$$dj_R/dV = j_R^*/V_R \quad [1]$$

Curve j_H' is the power requirement curve for water splitting derived from curves j_{H_2} and j_{O_2}, in Fig. 3a, by connecting points of equal anodic and cathodic currents to find the corresponding points of power requirement. Curve j_H is the power requirement curve shifted to include resistance losses through the solution bridge of the experimental device of this study. The maximum electrical efficiency is defined as

$$\eta_e^{max} = j_{sc}V_{oc}f/I = j_R^*V_R^*/I \quad [2]$$

where $j_R^*V_R^*$, the maximum power supplied by one PEC, is graphically depicted as the area of rectangle A (A_A). The light flux (W/cm^2) and fill factor are I and f, respectively. The maximum water splitting efficiency is

$$\eta_H^* = W_H\Delta G^\circ/INA = 1.23\, j_H^*/IN^* \quad [3]$$

where W_H is the hydrogen production rate (mol/s), ΔG° is the standard Gibbs free energy of formation for water (J/mol), and N is the number of panels. The power required is graphically depicted as the sum of the areas of rectan-

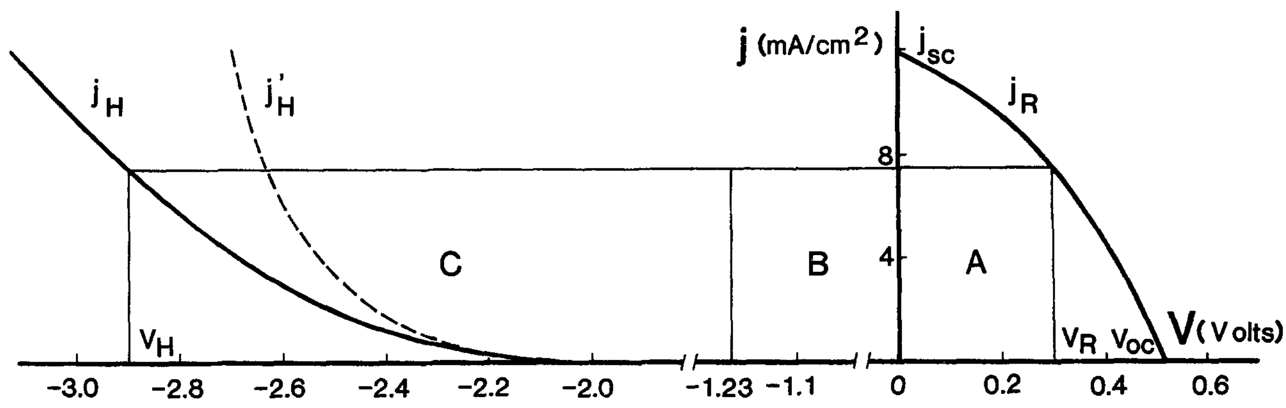

Fig. 4. Graphical method for determining optimum number of panels required for electrolysis. Curve j_R: power curve for CdSe in 1M polysulfide. Curve j_H: power requirement curve for water electrolysis on platinum electrodes including bridge and internal resistances of experimental device. Curve j'_H does not include bridge resistance.

gles B and C (A_B and A_C, respectively). A_B is the power available as Gibbs free energy of hydrogen evolution and $A_B/(A_B + A_C)$ is the ratio between hydrogen evolution and electrical efficiencies

$$\eta_H/\eta_e = 1.23/NV_R = 1.23/V_H \quad [4]$$

The optimum number of panels, N^*, can be determined from the areas of rectangles, A, B, and C for $j_H^* = j_R^*$

$$N^* = A_{C+B}/A_A = V_H^*/V_R^* \quad [5]$$

This method can be used for any electrolytic process, given the j-V data for the electrolytic process desired. Since the semiconductor surfaces are isolated from the end solution, the process can be carried out for any medium without a need to consider the type of semiconductor surface.

Experimental

The semiconductor face of the bipolar electrodes used in this study was fabricated by the method of Hodes *et al.* (10), by painting a slurry of CdSe on a titanium foil (0.025 mm thick) annealing in air at 500°C followed by photoetching in 0.1M H_2SO_4.

The CoS face was prepared by electroprecipitating $Co(OH)_2$ (11) from a $CoSO_4$ solution (20 g/liter, pH = 4) at 20-30 mA/cm^2 followed by a reductive treatment in a 1:1:1 sulfide-polysulfide-hydroxide solution at −1.2V *vs.* SCE. The terminal electrode faces were prepared by coating the Ti foil with a Pt film (*ca.* 350 nm thick) by RF sputtering with a Materials Research Company (Orangeburg, New York) Model 8620 sputtering apparatus.

The array device (Fig. 2) was identical to one used previously (2). A Pyrex tube having an inner diameter of 1.15 cm and a wall thickness of 0.118 cm was cut into segments at 45° angles. Six photoelectrodes were sandwiched between the segments with epoxy cement. A (dark) bipolar electrode was glued into a 90° cut. The terminal ends had gas collectors to monitor the volumes of gas evolved. Gas analysis was performed with a Varian Aerograph, Model 90-P using a column packed with 50g of 13X, 60-80-mesh sieves from Alltech Associates, Incorporated, with argon as the carrier gas at 30 ml/min.

The various polysulfide solutions were prepared by dissolving equimolar amounts of Na_2S and S in aqueous NaOH. The NaOH concentration in all the polysulfide solutions was 1M. The solution in the bridge and terminal compartments was 2M KOH.

Current-potential data were obtained with a Princeton Applied Research (PAR) Model 173 potentiostat/galvanostat, a PAR Model 175 universal programmer, and a Houston Instruments Model 2000 X-Y recorder. The illumination source was a 2500W xenon lamp. The lamp spectrum of the xenon lamp was measured with a monochromator (Jarrell Ash, Model 82560) and a radiometer (EG&G Princeton) Model 550. The equivalent solar power was determined by calculating the total solar flux required to obtain the bandgap light provided by the xenon lamp. The total light flux at the PEC and array device was measured with a surface adsorbing disk calorimeter (Scientech, Model 36-0203). The light intensity was varied with neutral density filters (Muffoletto Optical Company, Incorporated). Absorbances of polysulfide solutions were measured with a HP 8450A UV/VIS spectrophotometer. Solution and cell conductivities were measured with a Yellow Springs Instruments conductance meter, Model 32.

Results and Discussion

CdSe/polysulfide/CoS.—The effect of light flux.—The effect of light intensity and polysulfide concentration on the performance of a single PEC cell was experimentally studied. The results of this study were used to simulate the above effects on the performance of an array system. The light intensity was varied by one order of magnitude using neutral density filters. Power curves as a function of light intensity are given in Fig. 5a. The open dots indicate points of maximum power output. As can be seen from the dotted line, the potential corresponding to the maximum power

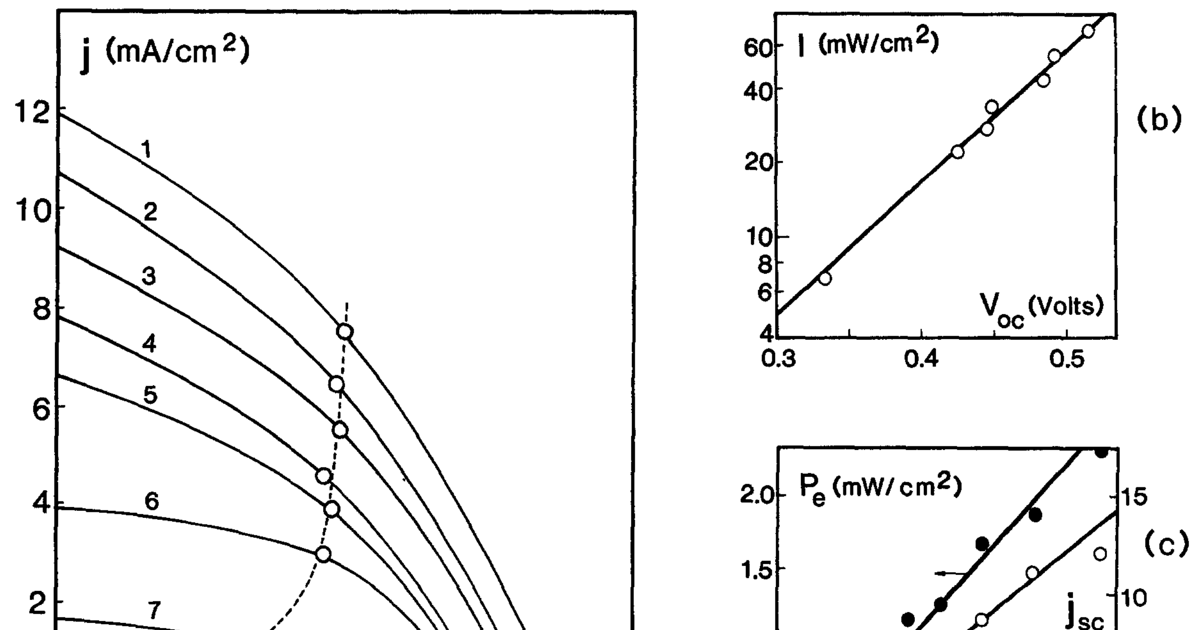

Fig. 5. Effect of light flux on electrical power output of a single PEC cell. (a) Power curves as a function of light intensities. Open points represent points of maximum power output. Polysulfide concentration: 1M. Effective solar flux densities (mW/cm^2) curve 1, 67; 2, 53.2; 3, 42.3; 4, 33.6; 5, 26.7; 6, 21.2; 7, 6.7. (b) Semilogarithmic plot of light flux density *vs.* open-circuit voltage. (c) Power output and short-circuit current *vs.* light flux density.

point is only weakly dependent on the light flux at intensities above 20 mW/cm^2. In Fig. 5B the logarithmic plot of light intensity *vs.* open-circuit voltage shows that the semiconductor is not saturated at the light fluxes used. Figure 5C shows that both the short-circuit current and the electrical power output are linearly related to the light flux.

Polysulfide concentration effects.—The polysulfide concentration (*e.g.*, S + S^{2-} taken as S_2^{2-}) was varied from 0.1 to 1.0*M*. One would expect that a decrease in the polysulfide concentration, an electrolyte which absorbs strongly in the visible, would have two opposing effects. While the light flux to the semiconductor surface would increase, there would be a negative effect on the mass transfer of reactants (S^{2-} and S_2^{2-}) to the electrodes. As can be seen in Fig. 6a and 6c, at concentrations higher than 0.60*M*, the power output is light limited. Above that concentration, the power output is linearly related to the light flux as shown in Fig. 5c. As the concentration is decreased, the BSP array becomes mass transfer controlled and the fill factor decreases as shown in Fig. 6b and by the flattening of the power curves in Fig. 6a. The dotted line in Fig. 6 shows that the potential at the maximum power point is weakly dependent on the redox couple concentration.

Simulation of bipolar CdSe-CoS PEC arrays.—The above data were used in a computer analysis of the type previously described, using j_{red}, j_{ox}, j_{H_2}, and j_{O_2} from experimental waves, to ascertain the effect of light intensity, redox couple concentration and number of panels on the efficiency of water splitting and electrical power generation and how these parameters are interrelated. Figure 7 shows the effect of light intensity on the efficiency of both simulated and experimental array devices operating with a 1:1:1 [S^{2-}]/[S]/[OH^-] electrolyte. A correction has been made for the light absorbed by the polysulfide solution and for the light reflected at the air-glass and glass-solution interfaces of the array device. The data show that the efficiency and the relationship between electrical and hydrogen production efficiency are not light intensity dependent. This is consistent with the data shown in Fig. 5a. The dotted line is the locus of optimum power points for a single panel at various light fluxes. At each light flux, additional curves can be obtained for a series array of panels. Such curves were measured at one light flux in a previous paper (2). With each additional panel added to the series, a new locus of optimum power points at various light fluxes is obtained. At the optimum number of panels, the locus of optimum power points above 20 mW/cm^2 has a very similar current-voltage dependence as the water splitting current-voltage data. Hence, the optimum number of panels is not light intensity dependent in the range 20-70 mW/cm^2. The data show that the method yields simulations in good agreement with experimental data.

Figure 8 shows the simulated hydrogen and electrical generation efficiencies for an array with 8 panels as a function of total sulfide concentration. The axis on the right gives actual uncorrected efficiencies. The axis on the left shows the efficiencies after correcting for light absorption and reflections. The absorption by the polysulfide solution in the experimental array is quite significant as the average path length through the solution is about 0.5 cm. A computer program was used to calculate average light fluxes, integrating over the photoanode surface area, considering the geometry of the arrangement of the panels. Hence, if an internal redox couple that gave the same V_{oc} and involved less absorbing species was used, an upper limit of

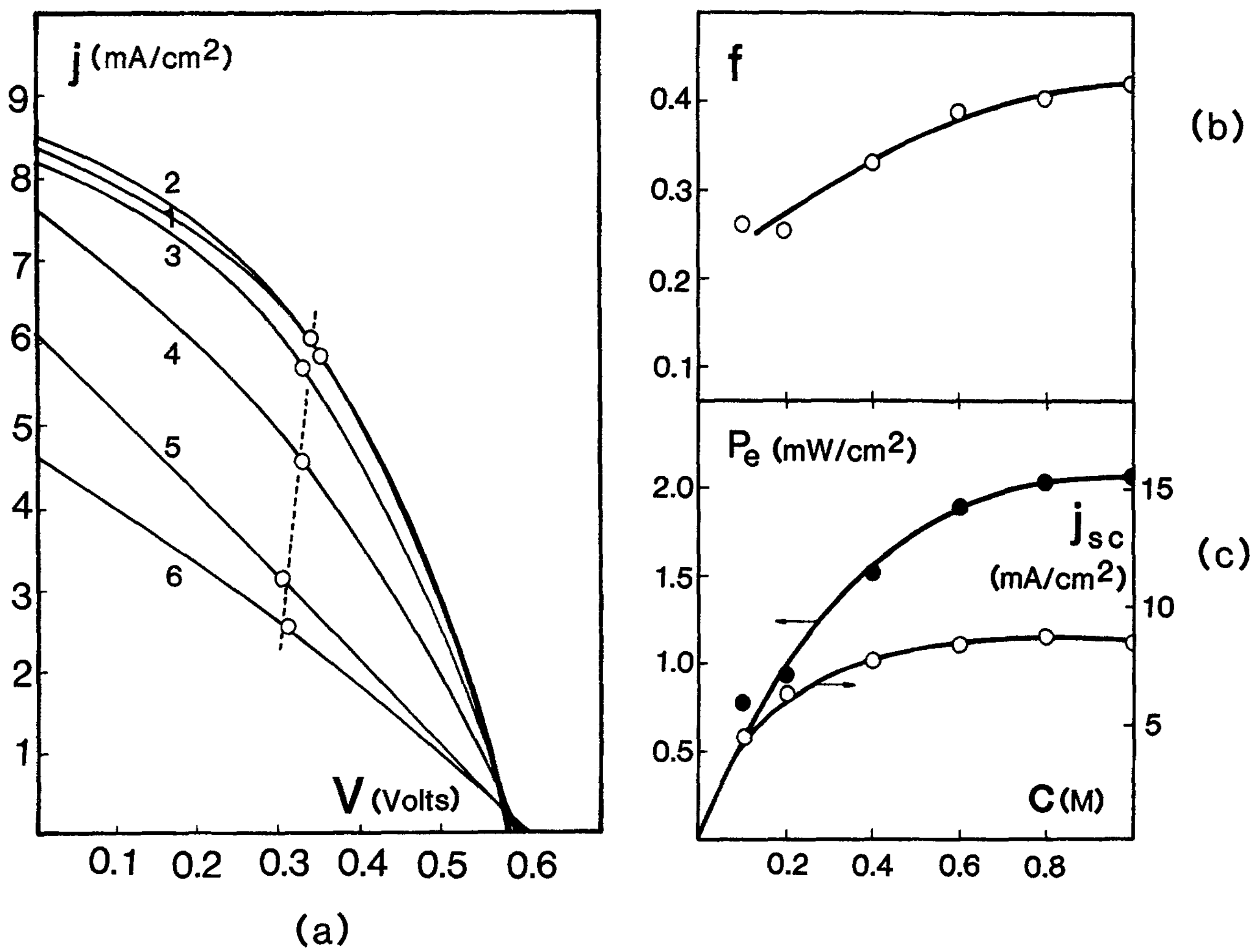

Fig. 6. Effect of polysulfide concentration on a single PEC cell output. Polysulfide (S^{2-} + S) concentration (*M*) and light flux at electrode surface (mW/cm^2): curve 1, 1.0, 49.0; 2, 0.8, 50.1; 3,0.6, 53.5; 4, 0.4, 57.0; 5, 0.2, 63.2; 6, 0.1, 67.5. (a) Power curves as a function of polysulfide concentration open points represent points of maximum power output. (b) Fill factor *vs.* concentration. (c) Power output and short-circuit current *vs.* concentration of polysulfide.

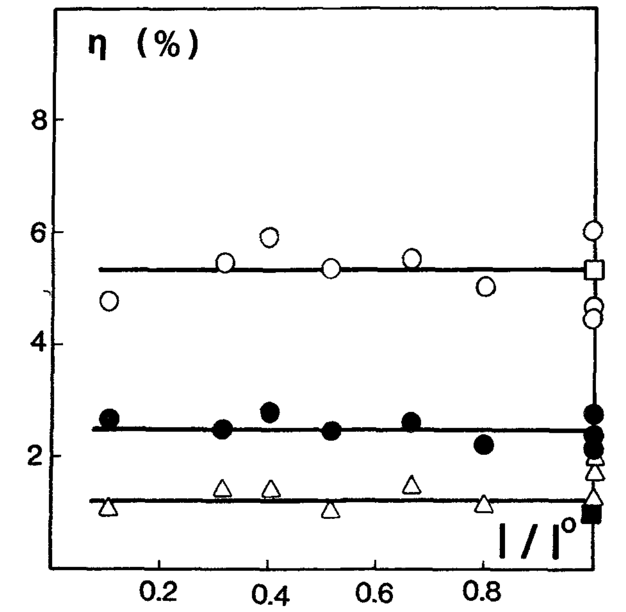

Fig. 7. Effect of light flux on electrical and water splitting efficiency of the BSP array system (I° = 67 mW/cm^2). (○) Calculated electrical efficiency of BSP array; (●) calculated water splitting efficiency of BSP array with 8 panels; (△) calculated water splitting efficiency of 6 panel BSP array; (□) experimental electrical efficiency of 6 panel system; (■) experimental water splitting efficiency of 6 panel system.

6% efficiency could be obtained with eight panels in the experimental device used in this study. Alternatively, with a miniblind type of array that minimizes the solution light path, using very narrow panels, the upper limit could be obtained, even with highly absorbing redox couples. Above 0.6*M* polysulfide the array is light limited and the efficiencies are weakly concentration dependent. Below 0.6*M* the array is mass transfer controlled.

The water splitting efficiency has been shown to be a function of the number of panels (Eq. [3]), attaining a maximum value. The efficiency is also concentration dependent. These relationships can be described as a surface in η-N-C space and is depicted in Fig. 9 as a two-dimensional projection, where each η-N curve corresponds to a given concentration. The solid dotted line in Fig. 8 is a cross sec-

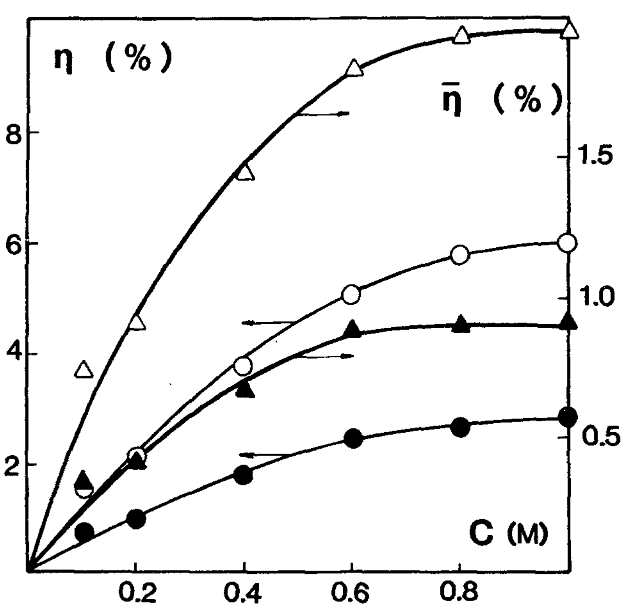

Fig. 8. Effect of polysulfide concentration on BSP array efficiencies. Left axis: (○) corrected electrical efficiencies; (●) corrected water splitting efficiency for 8 panel array. Right axis: (△) actual (uncorrected) electrical efficiency; (▲) actual (uncorrected) water splitting efficiency for 8 panel system.

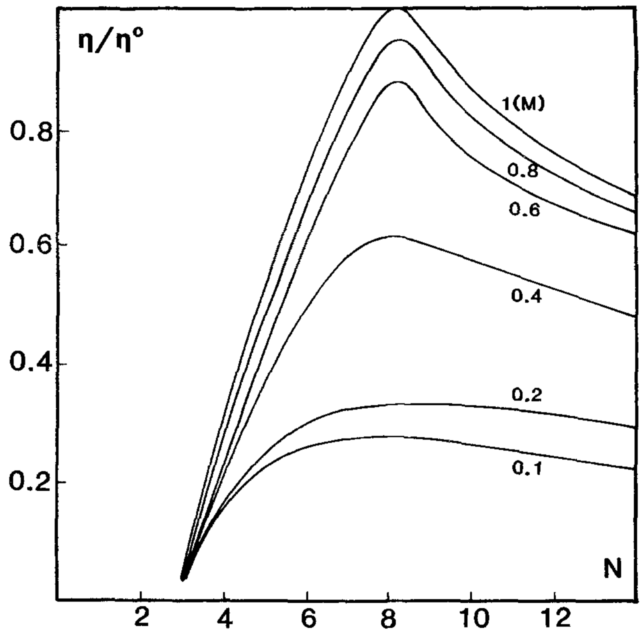

Fig. 9. Water splitting efficiency vs. number of panels at different total sulfide concentrations (η° = 0.028).

tion of Fig. 9 for N = 8. Although N is an integer, continuous curves are drawn for illustrative purposes. The curves in Fig. 9 show no dependence of the optimum number of panels on the concentration of the redox couple. This is consistent with the data in Fig. 6a. The dotted line is the locus of optimum power points as a function of redox couple concentration. Again, if series power curves are obtained with the optimum number of panels, this locus of points will spread out, resulting in a current-voltage curve similar to the water splitting current-voltage locus. Hence, the optimum number of panels is not concentration dependent.

Conclusions

The effect of light fluxes, polysulfide concentration, and number of CdSe//CoS panels on the electrical and hydrogen evolution efficiencies of an array system has been studied using a simple model requiring current-voltage data for a single photoelectrochemical cell and the power requirement curve for the desired electrolytic process.

We have shown that the optimum number of panels for water photolysis is neither dependent on light flux nor on the polysulfide concentration in the ranges studied. This optimum number in the array based on n-CdSe was between 8 and 9. The optimum polysulfide concentration was 0.8 to 1.0*M*. The system is not saturated at the light fluxes used (<70 mW/cm^2), and the electrical power output is linearly related to the light flux. Upper limits of 6 and 2.8% corrected electrical and water splitting efficiencies, respectively, have been obtained.

Efficiencies could be increased and the optimum number of panels reduced by using better catalytic surfaces for oxygen evolution, such as IrO_x or Fe-doped nickel oxide electrodes (12, 13), and by using smaller bandgap material. Such improvements are currently under investigation in these laboratories.

Acknowledgment

The support of this research by the Gas Research Institute (5982-260-0756) is gratefully acknowledged. We are grateful to the NATO Spanish Scientific Committee and CIRIT of Catalonia (Spain) for grants received by S.C.M. to carry out this research.

Manuscript submitted March 12, 1987; revised manuscript received Sept. 18, 1987.

The University of Texas assisted in meeting the publication costs of this article.

REFERENCES

1. E. S. Smotkin, A. J. Bard, A. Campion, M. A. Fox, T. Mallouk, S. E. Webber, and J. M. White, *J. Phys. Chem.*, **90**, 4606 (1986).
2. E. S. Smotkin, S. Cervera-March, A. J. Bard, A. Campion, M. A. Fox, T. Mallouk, S. E. Weber, and J. M. White, *ibid.*, **91**, 6 (1987).
3. A. Fujishima and K. Honda, *Nature (London)*, **238**, 37 (1972).
4. A. J. Bard, *Science*, **207**, 139 (1980).
5. H. Gerischer, in "Photoelectrochemistry, Photocatalysis and Photoreactors, Fundamentals and Developments," M. Schiavello, Editor, NATO ASI series, 146, 107 (1985).
6. R. Memming, in "Photoelectrochemistry, Photocatalysis and Photoreactors, Fundamentals and Developments," M. Schiavello, Editor, NATO ASI series, **146**, 107 (1985).
7. A. Heller, in "Energy Resources through Photochemistry and Catalysis," M. Graetzel, Editor, p. 385, Academic Press, New York (1983).
8. F.-R. F. Fan and A. J. Bard, *J. Am. Chem. Soc.*, **102**, 3677 (1980).
9. Y. I. Kharkats, E. D. German, V. E. Kazarinov, A. G. Pshenichnikov, and Y. V. Pleskov, *Int. J. Hydrogen Energy*, **11**, 617 (1986).
10. G. Hodes, D. Cahen, J. Manassen, and M. J. David, *This Journal*, **127**, 2252 (1980).
11. G. Hodes, J. Manassen, and D. Cahen, *ibid.*, **127**, 544 (1980).
12. B. V. Tidak, W. T. Lu, and J. E. Coleman, in "Comprehensive Treatise of Electrochemistry," J. O'M. Bockris, Editor, pp. 13-33, Plenum Press, New York (1981).
13. D. A. Corrigan, *This Journal*, **134**, 377 (1987).

Electrochemical Flue Gas Desulfurization

Reactions in a Pyrosulfate-Based Electrolyte

Kevin Scott,[1] Terry Fannon, and Jack Winnick*

School of Chemical Engineering, Georgia Institute of Technology, Atlanta, Georgia 30332

ABSTRACT

A new electrolyte has been found suitable for use in an electrochemical membrane cell for flue gas desulfurization (FGD). The electrolyte is primarily $K_2S_2O_7$ and K_2SO_4, with V_2O_5 as oxidation enhancer. This electrolyte has a melting point near 300°C which is compatible with flue gas exiting the economizer of coal-burning power plants. Standard electrochemical tests have revealed high exchange current densities, around 30 mA/cm^2, in the free electrolyte. Sulfur dioxide is found to be removed from simulated flue gas in a multiple-step process, the first of which is electrochemical reduction of pyrosulfate.

Electrochemical technology for gas separation has been used to remove trace amounts of contaminant gases and concentrate them into a by-product stream (1-4). An electrochemical driving force causes a net transfer of mass from a region of low concentration to a region of high concentration. A test cell operating on this principle has been found (5) to successfully remove and concentrate the sulfur dioxide in simulated power plant flue gas. This device utilized a ternary Li-Na-K sulfate eutectic (mp = 512°C) as the transport medium for the sulfur species. Sulfur dioxide is removed at the cathode and generated at high concentration at the anode with the net reactions

$$SO_2 + O_2 + 2e^- \rightarrow SO_4^{2-} \quad \text{cathode} \quad [1]$$

$$SO_4^{2-} \rightarrow SO_3 + 1/2\,O_2 + 2e^- \quad \text{anode} \quad [2]$$

The benefits of this molten salt electrochemical flue gas desulfurization cell include: high selectivity, no waste sludge production, one-step sulfur dioxide removal and recovery, and relatively easy expansion capability by cell stacking. However, the high operating temperature (>512°C) is incompatible with direct application to conventional power plants. The flue gases in a power plant leave the economizer at 250°-400°C (6), which is the ideal operating temperature range for the desulfurization device. A new, lower melting electrolyte must be identified. Alkali bisulfates have been studied (7), but lack sufficient thermal stability at the temperatures of interest. Here, we examine potassium pyrosulfate which is stable as a liquid in the desired temperature range. It is also widely available and inexpensive.

The commercial device would be configured like a stack of fuel cells, each with liquid electrolyte contained in a ceramic matrix. Ceramic gas-diffusion electrodes appear attractive as both cathode and anode [*e.g.*, Ref. (8)]. At the cathode, the sulfur dioxide and oxygen present in flue gas[2] must be converted into anions transportable to the anode (see Fig. 1). Here they are oxidized to sulfur trioxide and oxygen.

The process is quite similar to that in a molten carbonate fuel cell where the overall cathodic reaction is

$$CO_2 + 1/2\,O_2 + 2e^- = CO_3^{2-} \quad [3]$$

In a sulfate electrolyte, the overall cathode reaction, Eq. [1], was found to be limited only by gas-phase diffusion of the SO_2 (9). Proper cell design can provide economic operation even at 90% SO_2 removal (5).

At the lower temperatures, with potassium pyrosulfate as electrolyte, the cathodic reactions with sulfur dioxide and oxygen must be reinvestigated. In contrast with the sulfate electrolyte, no prior study seems available. Here we examine the electrochemical behavior of molten $K_2S_2O_7$ in contact with gases containing low levels of sulfur dioxide and oxygen. The effect of V_2O_5, a sulfur dioxide oxidation catalyst, is also explored. We focus on the cathodic processes, where the flue gas will act as oxidant, as these are expected to be rate limiting (10).

Experimental

Pyrex cell housings of various designs were employed to contain the molten electrode. One type is shown schematically in Fig. 2. The temperature was maintained at 340° ± 5°C in a custom-built furnace controlled by a double-pole

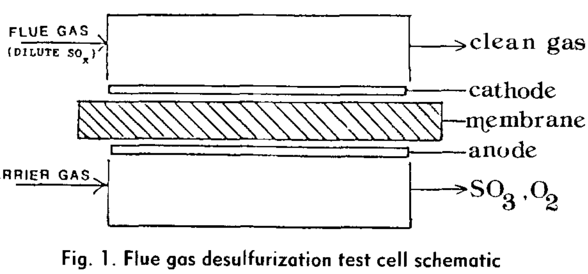

Fig. 1. Flue gas desulfurization test cell schematic

*Electrochemical Society Active Member.
[1]Present address: E.I. du Pont de Nemours and Company, Wilmington, Delaware.
[2]Typically 0.3% SO_2 and 3-5% O_2.